# Nonleaky and accelerated population transfer in a transmon qutrit

Xiao-Jing Lu,[1] M. Li,[1] Z. Y. Zhao,[1] Chun-Li Zhang,[1] Hong-Pei Han,[1] Zhi-Bo Feng,[1,*] and Yun-Qing Zhou[2,†]

[1]*School of Electric and Mechatronics Engineering, Xuchang University, Xuchang 461000, China*

[2]*Department of Physics, Key Laboratory of Oceanographic Big Data Mining & Application of Zhejiang Province, Zhejiang Ocean University, Zhoushan 316000, China*

(Received 15 June 2017; published 21 August 2017)

We propose a theoretical scheme for implementing nonleaky and accelerated population transfer with a transmon qutrit. For a transmon-regime artificial atom with weak level anharmonicity, the leakage effects on the target population transfer are considerable. Allowed by the level-transition rule, a two-photon resonant interaction can be obtained between the qutrit and microwave drivings. In the regime of large detuning, by adopting the technique of invariant-based inverse engineering, the population transfer with no leakage errors can be sped up drastically when compared with the adiabatic operation. Moreover, the accelerated operation is highly robust against decoherence effects. Thanks to these distinctive advantages, the proposed protocol could offer a promising avenue to optimal quantum operations on transmon artificial atoms.

DOI: 10.1103/PhysRevA.96.023843

## I. INTRODUCTION

Due to the potential applications to quantum information processing and state engineering, coherent controls of superconducting artificial atoms have attracted increasing attention in recent years [1–5]. The transmon-type superconducting quantum circuit, as one of the promising systems, is insensitive to the dephasing effect that is caused by the quantum fluctuations of gate charges and has a long coherence time [6–8]. Therefore, transmon quantum circuits offer us an excellent platform to study quantum information science [9–12] and to explore the basic laws of quantum mechanics [13–15]. However, transmon-type artificial atoms generally possess weak level anharmonicity [6,16], namely, the two nearest level spacings are closed to each other. When the artificial atoms interact with external driving fields, the weak level anharmonicity could give rise to considerable leakage effects [9,17,18], which are detrimental to implementation of high-fidelity quantum operations [19]. By the technique of pulse shaping and control optimization, some smart approaches have been put forward to reduce the leakage effects [20–22].

Stimulated Raman adiabatic passage (STIRAP) is a powerful approach to coherently control quantum systems [23,24]. Based on the method of STIRAP, many quantum operations on superconducting artificial atoms have been investigated both theoretically and experimentally [19,25–27]. However, the adiabatic processes generally need long evolution times. Especially, when the times are comparative or longer than the decoherence times of the systems, the adiabatic operations become undesirable. Thus, how to realize the fast quantum coherent operation is a significant issue in the practical context [28–33]. As a promising technique, a shortcut to adiabaticity (STA) including inverse engineering [34,35], transitionless quantum driving [36,37], and fast-forward approaches [38] can realize the same target operation with the adiabatic process but within a shorter time. In two- and three-level systems, inverse engineering has been used extensively to realize adiabatic population transfers [39–44]. Very recently, the technique of transitionless quantum driving has been adopted for fast quantum information processing with superconducting artificial atoms [45,46], which prove that the shortcut approach is effective and robust against the decoherence effects of superconducting qubits.

In this paper, we apply the inverse engineering method to perform a nonleaky and accelerated population transfer within a transmon-type qutrit. Due to the weak level anharmonicity of the artificial atom, the leakage effects induced by the resonant drivings are considerable. A qutrit, constituted by the first three levels of the system, can be coupled to the microwave drivings, consisting of ac gate voltage and time-dependent bias flux. Allowed by the level-transition rule, we address a $\Lambda$-configuration interaction. In the case of two-photon resonance with a large detuning, the nonleaky population transfer can be obtained effectively. By the method of invariant-based inverse engineering, the population transfer can be accelerated remarkably in contrast with the STIRAP-like adiabatic operation. Thanks to a shorter evolution time, the accelerated operation is more robust against decoherence effects. Consolidating the negligible leakage effect with fast coherent control, the present protocol could offer a potential way for realizing optimal population transfer with transmon quantum circuits.

This paper is organized as follows. In Sec. II, we present a transmon-type artificial atom with weak level anharmonicity. Section III demonstrates the quantum leakages induced by resonant drivings during the state inversions. In Sec. IV, transferring population with negligible leakages can be drastically sped up within a qutrit. Finally, discussion and a conclusion are drawn in Sec. V.

## II. A TRANSMON-TYPE ARTIFICIAL ATOM WITH WEAK LEVEL ANHARMONICITY

As schematically shown in Fig. 1(a), we consider a transmon-type Cooper-pair box (CPB) circuit. The CPB contains a superconducting box with $n$ extra Cooper pairs, and the charging energy scale of the system is $E_c$. Through two symmetric Josephson junctions (with the identical coupling

*zbfeng010@163.com

†zhouyunqing@zjou.edu.cn

 

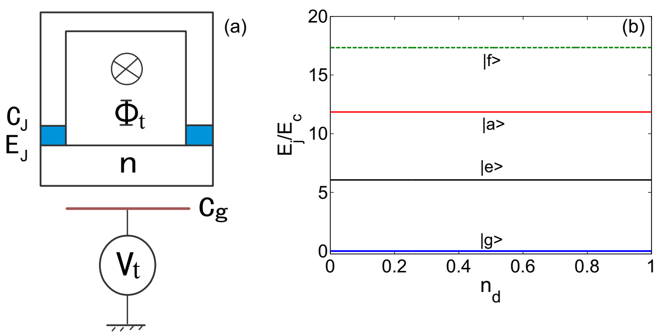


FIG. 1. (a) Schematic diagram of a transmon-regime quantum circuit. (b) The first four eigenlevels $E_j$ (in units of $E_c$) of the transmon system vs the static gate charge $n_d$, with $j = g, e, a$, and $f$. Here the system parameters are $E_c/\hbar = 2\pi \times 1.05$ GHz and $E_{Jd} = 20E_c$. Level states $|g\rangle$, $|e\rangle$, $|a\rangle$, and $|f\rangle$ are chosen at $n_d = 0.5$, and $E_g$ has been taken as the zero-energy reference.

energies $E_J$ and capacitances $C_J$), the CPB is connected to a segment of a superconducting loop. In the transmon regime, the characteristic system parameter $E_J$ is generally one order of magnitude larger than $E_c$ [6].

A total voltage bias $V_t = V_d + \tilde{V}_s$, consisting of a static voltage $V_d$ and an ac microwave driving $\tilde{V}_s = V_s\cos(\omega_s t)$, is applied to the CPB through a gate capacitance $C_g$ [47,48], where the amplitude $V_s$ is controllable, and $\omega_s$ stands for the corresponding microwave frequency. A magnetic flux $\Phi_t = \Phi_d + \tilde{\Phi}_p$ can be applied to the superconducting loop [49–51], in which $\Phi_d$ is a static flux, and $\tilde{\Phi}_p = \Phi_p\cos(\omega_p t)$ denotes a time-dependent flux [4], with $\Phi_p$ being the amplitude and $\omega_p$ being the microwave frequency. Note that the amplitude $V_s$ ($\Phi_p$) is much smaller than $V_d$ ($\Phi_d$) in the present scheme.

In the absence of the microwave drivings $\tilde{V}_s$ and $\tilde{\Phi}_p$, the static CPB system is described by the Hamiltonian $H_0 = E_c(n - n_d)^2 - E_{Jd}\cos\theta$, where the first term is the charging energy, with $E_c = 2e^2/C_t$. The polarized gate charge induced by $V_d$ is $n_d = C_g V_d/2e$, and $E_{Jd} = 2E_J\cos(\pi\frac{\Phi_d}{\Phi_0})$ is the effective Josephson energy, in which $\Phi_0$ indicates the flux quantum. Within the basis of Cooper-pair number states $\{|n\rangle,|n+1\rangle\}$, the above Hamiltonian can be formally rewritten as

$$H_0 = \sum_n \left[E_c(n-n_d)^2|n\rangle\langle n| - \frac{E_{Jd}}{2}(|n\rangle\langle n+1| + \text{H.c.})\right]. \tag{1}$$

According to Eq. (1), we can obtain the eigenlevels and eigenstates of the static transmon system. The four lowest levels $E_j$ versus $n_d$ are plotted in Fig. 1(b), with $j = g, e, a$, and $f$. Apparently, these levels are insensitive to the fluctuation of charge number $n_d$, which thus contribute to prolong the coherence time of the transmon system. At a working point of $n_d = 0.5$, we select four eigenstates $|j\rangle$ under consideration, in which each state can be written as a superposition of Cooper-pair number states, i.e., $|j\rangle = \sum_n c_{jn}|n\rangle$, with $c_{jn}$ being the superposition coefficients. From Fig. 1(b), it is obvious that the transmon system has a weak level anharmonicity, namely, energy spacings $E_e - E_g$, $E_a - E_e$, and $E_f - E_a$ are closed to each other. The weak anharmonicity of the transmon system could have considerable effects on the coherent dynamical evolution, as mentioned below.

## III. LEAKAGE EFFECTS INDUCED BY RESONANT DRIVING IN THE COHERENT OSCILLATIONS

The interaction between the CPB and the ac microwave voltage $\tilde{V}_s$ reads [47,48]

$$H_s = -2E_c\sum_n \tilde{n}_s(n-n_d)|n\rangle\langle n|, \tag{2}$$

in which $\tilde{n}_s = C_g\tilde{V}_s/2e$, and the fast oscillating term of $\tilde{n}_s^2$ with higher frequency has been neglected under the rotation wave approximation (RWA). Clearly, within the basis of $\{|n\rangle,|n+1\rangle\}$, $H_s$ has a diagonal coupling form. The magnetic coupling between the CPB system and the bias flux $\tilde{\Phi}_p$ is given by

$$H_p = -\frac{E_{Jp}}{2}\sum_n(|n\rangle\langle n+1| + \text{H.c.}). \tag{3}$$

Since the amplitude of $\tilde{\Phi}_p$ is much smaller than $\Phi_0$, we have $\cos(\pi\frac{\tilde{\Phi}_p}{\Phi_0}) \approx 1$ and $\sin(\pi\frac{\tilde{\Phi}_p}{\Phi_0}) \approx \pi\frac{\tilde{\Phi}_p}{\Phi_0}$. In this case, the Josephson coupling determined by the time-dependent bias flux becomes $E_{Jp} = 2E_J\frac{\pi\tilde{\Phi}_p}{\Phi_0}\sin(\pi\frac{\Phi_d}{\Phi_0})$. Different from $H_s$, the interaction $H_p$ is a nondiagonal form $|n\rangle\langle n+1|$.

In what follows, by analyzing the coherent population inversions, we focus on the driving-induced leakage errors that are associated with the weak level anharmonicity. As an exemplified case, an ac microwave driving $\tilde{V}_s$ is applied to the considered CPB [see Figs. 2(a) and 2(b)]. The microwave field, having a frequency $\omega_s$ which is resonantly matched with transition frequency $\omega_{eg} = (E_e - E_g)/\hbar$, aims at inducing the target transition between $|g\rangle$ and $|e\rangle$. However, because of the weak level anharmonicity, there exist small detunings $\Delta_{ea} = \omega_s - \omega_{ae}$ and $\Delta_{af} = \omega_s - \omega_{fa}$, with $\omega_{ae} = (E_a - E_e)/\hbar$ and $\omega_{fa} = (E_f - E_a)/\hbar$. As a result, the unwanted transitions $|e\rangle \longleftrightarrow |a\rangle$ and $|a\rangle \longleftrightarrow |f\rangle$ are also triggered by $\tilde{V}_s$ simultaneously, which are referred to as quantum leakages beyond the considered subspace $\{|g\rangle,|e\rangle\}$. For the different initial states $|g\rangle$ and $|e\rangle$, as given in Figs. 2(a) and 2(b), the coherent oscillations between $|g\rangle$ and $|e\rangle$ are considered, respectively. Here we concentrate on the leakages, which can be characterized by the populations occupied by $|a\rangle$ and $|f\rangle$ [19].

Through numerically solving the time-dependent Schrödinger equation, we deal with the coherent population dynamics. For an arbitrary state vector, $\psi(t) = \sum_j c_j(t)|j\rangle$, where $c_j(t)$ are the normalization coefficients, we can get their time evolutions which satisfy the following equation:

$$i\hbar\frac{d}{dt}\begin{bmatrix}c_g(t)\\c_e(t)\\c_a(t)\\c_f(t)\end{bmatrix} = \begin{bmatrix}E_g & t_{ge} & 0 & 0\\ t_{ge}^* & E_e & t_{ea} & 0\\ 0 & t_{ea}^* & E_a & t_{af}\\ 0 & 0 & t_{af}^* & E_f\end{bmatrix}\begin{bmatrix}c_g(t)\\c_e(t)\\c_a(t)\\c_f(t)\end{bmatrix}, \tag{4}$$

where $t_{ge}$, $t_{ea}$, and $t_{af}$ are the corresponding transition matrix elements. According to Eq. (2), we get the coupling matrix element $t_{ge} = \langle g|H_s|e\rangle = -2E_c n_s O_{ge}\cos(\omega_s t)$, where $n_s = C_g V_s/2e$ indicates the ac voltage amplitude, and $O_{ge} = \sum_n c_{gn}^* c_{en}(n-n_d)$ is the overlap between $|g\rangle$ and $|e\rangle$ at the

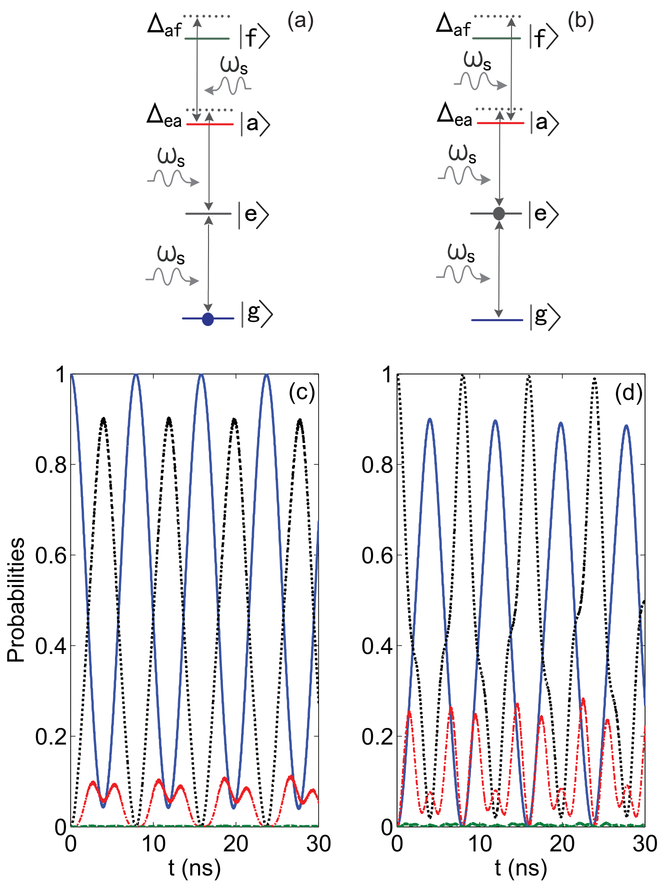

FIG. 2. Under a microwave field $\tilde{V}_s$ with a resonant frequency $\omega_s = \omega_{eg}$, the leakage effects on the level transition $|g\rangle \leftrightarrow |e\rangle$ of interest in the four-level system with the different initial states $|g\rangle$ (a) and $|e\rangle$ (b). The coherent dynamical population vs time (c) with initial state $|g\rangle$ (blue solid line) and (d) with initial state $|e\rangle$ (black dotted line); the populations of $|a\rangle$ (red dash-dotted line) and $|f\rangle$ (green dashed line) represent the leakage effects.

working point of $n_d$. Similarly, the transition matrix element between $|e\rangle$ ($|f\rangle$) and $|a\rangle$ that is caused by the same driving $\tilde{V}_s$ is $t_{ea} = -2E_c n_s O_{ea} \cos(\omega_s t)$ $[t_{af} = -2E_c n_s O_{af} \cos(\omega_s t)]$, respectively, with $O_{ea} = \sum_n c^*_{en} c_{an}(n - n_d)$ and $O_{af} = \sum_n c^*_{an} c_{fn}(n - n_d)$ being the wave-function overlaps.

Here the voltage amplitude is chosen as a constant, $n_s = 0.05$. At the working point $n_d = 0.5$, we have $O_{ge} = -1.231$, $O_{ea} = -1.700$, and $O_{af} = -2.024$, respectively. The coherent evolution of the system can be simulated by numerically calculating Eq. (4). For the different initial states, the coherent evolutions with time are plotted in Figs. 2(c) and 2(d), respectively. Due to the weak level anharmonicity, the probabilities $P_a$ and $P_f$ occupied by $|a\rangle$ and $|f\rangle$, acting as leakage errors, appear in the system driven by the resonant driving with $\omega_s = \omega_{eg}$. To quantitatively demonstrate the leakage effect, we take the infidelity of population transfer as in [48], $F_{\rm in} = 1 - |\langle\psi|\psi_i\rangle|^2$, where $|\psi\rangle$ is the realistic state with the leakage effect, and $|\psi_i\rangle$ is the ideal one. Ideally, it is found that the initial state $|g\rangle$ ($|e\rangle$) will be completely converted to $|e\rangle$ ($|g\rangle$) after a duration time $t_{ex} \simeq 3.85$ ns. However, when taking into account the leakage effects, the realistic state $|\psi(t_{ex})\rangle$ is occupied by $|e\rangle$ ($|g\rangle$) with a probability $P_e \simeq 90.05\%$

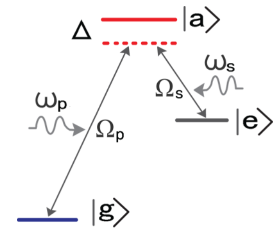

FIG. 3. In the case of two-photon resonance with a large detuning $\Delta$, a $\Lambda$-type interaction between the qutrit and the microwave drivings with frequency $\omega_p$ and $\omega_s$, and the Rabi couplings are $\Omega_p$ and $\Omega_s$, respectively.

($P_g \simeq 89.80\%$), as shown in Figs. 2(c) and 2(d), respectively. Then the infidelities are $F_{\rm in} = 9.95$ and $10.20\%$, respectively. Thereby, the leakage effects induced by the resonant driving are significant.

As mentioned in [19], the leakage effects are closely associated with the weak level anharmonicity. Compared with $\Delta_{ea}$, an increased detuning $\Delta_{af}$ sharply weakens the $\tilde{V}_s$ -induced dynamical transition between $|a\rangle$ and $|f\rangle$. It is found that the $P_f$ is much smaller than $P_a$ during the coherent evolutions in both Figs. 2(c) and 2(d). Thus the influence of population occupied by $|f\rangle$ on the coherent transfer between $|g\rangle$ and $|e\rangle$ of interest can be neglected here. As a result, we need to focus on the dynamical evolution within the first three levels, which constitute our qutrit under consideration. It is worth noting that the following approach for transferring the target states $|g\rangle$ and $|e\rangle$ can remove the leakage effects originating from the higher level states $|a\rangle$ and $|f\rangle$.

## IV. NONLEAKY AND ACCELERATED POPULATION TRANSFER

In the chosen qutrit, as demonstrated in Fig. 3, we first address how to realize robust population transfer by eliminating the considerable leakage errors. The $\tilde{V}_s$-induced coupling between $|e\rangle$ and $|a\rangle$ is described by $\langle e|H_s|a\rangle = \Omega_s \cos(\omega_s t)$, where

$$\Omega_s = -2E_c n_s O_{ea} \tag{5}$$

acts as the Rabi coupling strength. Owing to the prohibition by the parity-symmetry determined selection rule, the electric interaction $H_s$ with a diagonal coupling form does not cause the transition between $|g\rangle$ and $|a\rangle$. However, allowed by the level-transition rule, the magnetic interaction Hamiltonian $H_p$ can give rise to the wanted coupling between $|g\rangle$ and $|a\rangle$, $\langle g|H_p|a\rangle = \Omega_p \cos(\omega_p t)$, in which

$$\Omega_p = -E_J \pi \frac{\Phi_p}{\Phi_0} \sin\left(\pi \frac{\Phi_d}{\Phi_0}\right) O_{ga} \tag{6}$$

denotes the Rabi coupling, with $O_{ga} = \sum_n c^*_{gn} c_{an} \langle n|(|n\rangle\langle n+1| + \text{H.c.})|n\rangle$ being the overlap between $|g\rangle$ and $|a\rangle$.

We construct an efficient way to implement population transfer between the target states $|g\rangle$ and $|e\rangle$ . By applying two microwave drivings $\tilde{\Phi}_p$ and $\tilde{V}_s$, the couplings $|g\rangle \longleftrightarrow |a\rangle$ and $|e\rangle \longleftrightarrow |a\rangle$ can be realized, respectively. Within the basis of $\{|g\rangle, |a\rangle, |e\rangle\}$, a $\Lambda$-configuration interaction under the reference frame rotating at frequencies $\omega_p$ and $\omega_s$ can be given by

$$H_I = \frac{\hbar}{2}\begin{pmatrix} 0 & \Omega_p & 0 \\ \Omega_p & 2\Delta & \Omega_s \\ 0 & \Omega_s & 0 \end{pmatrix}, \tag{7}$$

where the RWA has been adopted, and we consider the two-photon resonance, i.e., $\Delta = \omega_{ag} - \omega_p = \omega_{ae} - \omega_s$. In the regime of large detuning $\Delta \gg \Omega_{p,s}$, level state $|a\rangle$ is scarcely populated ($c_a \simeq 0$) during the population transfer $|g\rangle \longleftrightarrow |e\rangle$. As a consequence, the leakage effect can be eliminated naturally. After adiabatically eliminating the auxiliary state $|a\rangle$, a reduced two-level system in the subspace $\{|g\rangle,|e\rangle\}$ can be obtained as [39,52]

$$H_e = \frac{\hbar}{2}\begin{pmatrix} -\Delta_e & \Omega_e \\ \Omega_e & \Delta_e \end{pmatrix}, \tag{8}$$

where the effective detuning $\Delta_e$ and Rabi frequency $\Omega_e$ are

$$\Delta_e = \frac{\Omega_p^2 - \Omega_s^2}{4\Delta}, \quad \Omega_e = -\frac{\Omega_p\Omega_s}{2\Delta}. \tag{9}$$

Based on Hamiltonian (8), we use the inverse engineering method to design the following STA.

Associated with the time-dependent Hamiltonian, there are Hermitian dynamical invariants $I$, fulfilling $\partial I/\partial t + (1/i\hbar)[I,H_e] = 0$, so that their expectation values remain constant. Here $I$ could be parametrized as

$$I = \frac{\hbar}{2}\Omega_0\begin{pmatrix} \cos\theta & \sin\theta e^{-i\beta} \\ \sin\theta e^{i\beta} & -\cos\theta \end{pmatrix}, \tag{10}$$

where $\Omega_0$ is an arbitrary constant frequency to keep $I$ with dimension of energy, and $\theta = \theta(t)$ and $\beta = \beta(t)$ are time-dependent angles. Using the invariant condition, we have the differential equations as

$$\begin{aligned} \dot\theta &= -\Omega_e \sin\beta, \\ \dot\beta &= -\Omega_e \cot\theta\cos\beta - \Delta_e. \end{aligned} \tag{11}$$

The eigenstates $|\phi_n(t)$ and eigenvalues $\lambda_n$ of the invariant $I$ satisfy $I(t)|\phi_n(t)\rangle = \lambda_n|\phi_n(t)\rangle$, with $n = \pm$ and $\lambda_\pm = \pm\hbar\Omega_0/2$ . Consistently, the normalized eigenstates can be written as

$$|\phi_+(t)\rangle = \begin{pmatrix} \cos\frac{\theta}{2}e^{-i\beta} \\ \sin\frac{\theta}{2} \end{pmatrix}, \quad |\phi_-(t)\rangle = \begin{pmatrix} \sin\frac{\theta}{2} \\ -\cos\frac{\theta}{2}e^{i\beta} \end{pmatrix}. \tag{12}$$

According to Lewis-Riesenfeld theory [53], the solution of the time-dependent Schrödinger equation, up to a global phase factor, can be expressed as

$$|\psi(t)\rangle = \Sigma_n a_n e^{i\gamma_n(t)}|\phi_n(t)\rangle,$$

where $a_n$ are time-independent amplitudes, and Lewis-Riesenfeld phases are $\gamma_n(t) \equiv \frac{1}{\hbar}\int_{t_i}^{t}\langle\phi_n(t')|i\hbar\frac{\partial}{\partial t'} - H_e(t')|\phi_n(t')\rangle dt'$, and the initial time is chosen as $t_i = 0$.

Now we utilize the inverse engineering of population inversion based on dynamical invariant. The initial and final states of the process are set as $|\psi(0)\rangle = |g\rangle \equiv \binom{0}{1}$ and $|\psi(T)\rangle = |e\rangle \equiv \binom{1}{0}$, respectively. The state trajectory between them may be parametrized according to one of the eigenstates $|\phi_n(t)\rangle$ of the invariant. By using $|\phi_+(t)\rangle$ in Eq. (12), the boundary conditions satisfy

$$\theta(0) = \pi, \;\; \theta(T) = 0, \tag{13}$$

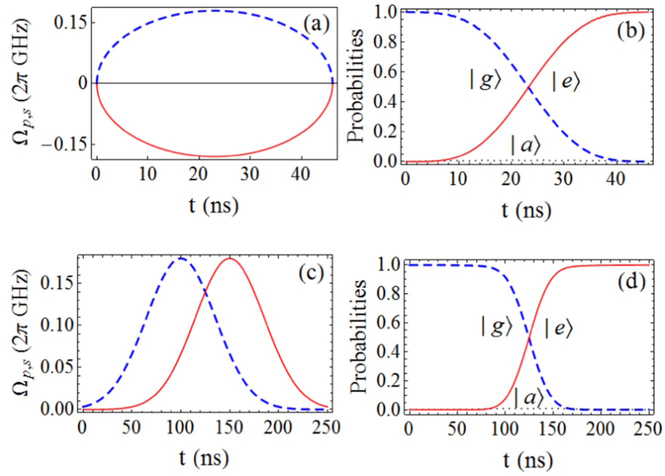


FIG. 4. (a) The designed Rabi couplings $\Omega_p$ (blue dashed line) and $\Omega_s$ (red solid line) vs time $t \in [0,\ 46\ \text{ns}]$. (b) The population transfer via the STA. (c) The Gaussian pulses in the STIRAP as functions of time, $\Omega_p$ (blue dashed line) and $\Omega_s$ (red solid line). (d) The Gaussian pulse-induced adiabatic population transfer from $|g\rangle$ to $|e\rangle$.

which guarantees the desired initial and final states. Meanwhile,

$$\dot\theta(0) = 0, \;\; \dot\theta(T) = 0, \tag{14}$$

which makes $\Omega_e(0) = \Omega_e(T) = 0$. And thus $H_e(t)$ and $I(t)$ commute at both times $t = 0$ and $T$. Apart from the boundary conditions, $\theta(t)$ and $\beta(t)$ are in principle quite arbitrary. We give the ansatz

$$\theta(t) = \sum_{k=0}^{3} a_k t^k, \quad \beta(t) = \sum_{k=0}^{4} b_k t^k, \tag{15}$$

where $a_k$ are determined by the conditions (13) and (14), and $b_k$ satisfies the following conditions:

$$\begin{aligned} &\beta(0) = -\pi/2, \beta(T/2) = -\pi/2, \\ &\beta(T) = -\pi/2, \dot\beta(T/2) = 0, \\ &\dot\beta(T) = 0. \end{aligned} \tag{16}$$

From Eq. (9), $\Omega_p$ and $\Omega_s$ can be solved as

$$\begin{aligned} \Omega_p(t) &= 1.414\sqrt{\Delta[\Omega(t) + \Delta_e(t)]}, \\ \Omega_s(t) &= \frac{\Omega_p(t)[\Omega(t) - \Delta_e(t)]}{\Omega_e(t)}, \end{aligned} \tag{17}$$

where $\Omega(t) = \sqrt{\Omega_e^2(t) + \Delta_e^2(t)}$, and $\Omega_e$ and $\Delta_e$ can be got from Eq. (11). The polynomial ansatz in Eq. (15) is designed for the Hamiltonian (8). Here we choose detuning $\Delta = 1.0 \times 2\pi$ GHz. Based on the polynomial ansatz in Eq. (15), we show the dependencies of $\Omega_p$ and $\Omega_s$ on time in Fig. 4(a), and the corresponding population transfer in Fig. 4(b). For the given parameters, the population transfer from $|g\rangle$ to $|e\rangle$ is realized within about 46 ns. During the transfer process, the population of $|a\rangle$ is zero. Here we reduce the three-level system in the two-photon resonance into an effective two-level system, and design the adjustable parameters for the effective two-level system. And we find the designed Rabi couplings (17) can realize a nonleaky and fast population transfer.

In order to compare the evolution time with that of the STIRAP process, we analyze the coherent evolution of the system driven by two Gaussian pulses [52],

$$\Omega_p^{(G)} = \Omega_{p0} e^{-(t-\tau_p)^2/\tau^2},$$

$$\Omega_s^{(G)} = \Omega_{s0} e^{-(t-\tau_s)^2/\tau^2},$$

as shown in Fig. 4(c). Physically, we select the static working points $n_d = 0.5$ and $\Phi_d = 0.265\Phi_0$, then the overlap induced by the magnetic interaction is $O_{ga} = -0.216$. Here the microwave amplitudes are chosen as $n_s = 0.05$ and $\Phi_p = 0.023\Phi_0$. When $E_J = 15E_c$, we thus have $\Omega_{p0} = \Omega_{s0} \simeq 0.18 \times 2\pi$ GHz, which are equal to the values of $\max(\Omega_p, |\Omega_s|)$ in Fig. 4(a). And the other parameters are $\tau_p = 100$ ns, $\tau_s = 150$ ns, and $\tau = 50$ ns, with a duration time $t \in [0, 250$ ns]. Driven by the Gaussian pulses, the coherent population transfer from the initial state $|g\rangle$ to the final state $|e\rangle$ can be performed after a long evolution time, as given in Fig. 4(d). In spite of no population of $|a\rangle$, the adiabatic evolution takes a time much longer than that of the shortcut evolution we designed. Therefore, compared with the technique of STIRAP for population transfer, the present STA protocol greatly shortens the transfer time, which is very helpful to speed up quantum operations on the transmon artificial atoms.

As a practical issue related to quantum operation, the system evolution becomes dissipative owing to the decoherence effects originated from energy relaxation and dephasing. Next, based on the standard dissipation theory, we treat the decoherence effects on the population transfer. The reduced density matrix regarding $|g\rangle$ and $|e\rangle$ is $\rho$, the dynamical evolution of which can be described by the Lindblad-type master equation

$$\frac{d\rho}{dt} = -i[H_e,\rho] + \gamma D[\sigma_-]\rho + \frac{\gamma_\varphi}{2} D[\sigma_z]\rho, \tag{18}$$

where $H_e$ denotes the effective Hamiltonian that governs the system evolution subject to no decoherence effects, $\gamma$ and $\gamma_\varphi$ are the relaxation and dephasing rates associated with states $|g\rangle$ and $|e\rangle$, respectively, and $D[L]\rho = (2L\rho L^\dagger - L^\dagger L\rho - \rho L^\dagger L)/2$, with $L = \sigma_-$ and $\sigma_z$. The inversion operator is defined as $\sigma_- = |g\rangle\langle e|$, and the Pauli operator reads $\sigma_z = |e\rangle\langle e| - |g\rangle\langle g|$.

To characterize the decoherence effects on the population transfer, we adopt the fidelity as [54]

$$F = \langle\psi_i(t_{ex})|\rho|\psi_i(t_{ex})\rangle, \tag{19}$$

in which $|\psi_i(t_{ex})\rangle$ is an ideal state at a given time $t = t_{ex}$, and $\rho = |\psi(t_{ex})\rangle\langle\psi(t_{ex})|$ denotes the density matrix with respect to the realistic state $|\psi(t_{ex})\rangle$. Here $t_{ex}$ stands for a duration time for a complete population inversion. In the shortcut case, by numerically solving Eqs. (18) and (19), we acquire the fidelity $F$ of the transfer from $|g\rangle$ to $|e\rangle$ after an evolution time $t_{ex} = 46$ ns, which is a function of the rates $\gamma$ and $\gamma_\varphi$ (see Fig. 5). It is found that the fidelity can reach up to $F = 98.71\%$ for the experimentally accessible rates $\gamma/2\pi = 0.08$ MHz and $\gamma_\varphi/2\pi = 0.07$ MHz [55]. Even for the larger decay rates $\gamma/2\pi = 0.3$ MHz and $\gamma_\varphi/2\pi = 0.3$ MHz, we have a robust transfer with $F = 95.24\%$. Therefore, the speed-up transfer is not typically sensitive to the increases of decay rates just due to the time-shortened process.

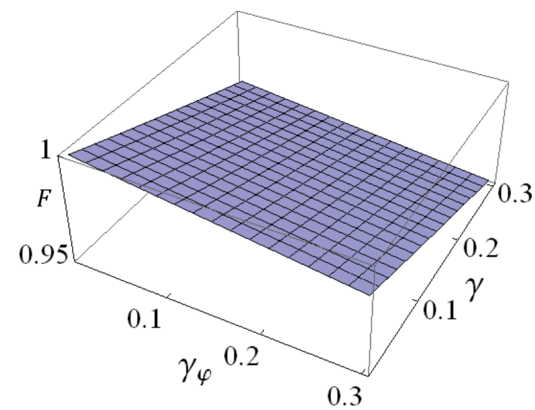


FIG. 5. The accelerated transfer fidelity $F$ vs the relaxation rate $\gamma$ and dephasing rate $\gamma_\varphi$ (in units of $2\pi$ MHz).

## V. DISCUSSION AND CONCLUSION

The present protocol is also applicable to the performance of the inverse population transfer, namely, the inversion from the initial state $|e\rangle$ to the target state $|g\rangle$. To this end, only by changing the Rabi frequency $\Omega_s$ to $-\Omega_s$ while keeping $\Omega_p$ fixed, the inversion from $|e\rangle$ to $|g\rangle$ can be accomplished backwards in our scenario. Here $\Omega_s$ depends on the charge number $n_s$, which is determined by the controllable voltage $V_s$. As a consequence, the bidirectional state transfer between $|g\rangle$ and $|e\rangle$ is flexible only by adjusting $V_s$, which can significantly reduce complexity of experimental manipulation. The reversible population transfer could have a wide application to coherent control, quantum computation, and information processing.

The proposed scheme may have the following characteristics and advantages.

(i) As a necessary requirement in our scenario, the large detuning $\Delta$ can guarantee no level transitions caused by $\tilde{\Phi}_p$ or $\tilde{V}_s$ solely. In the regime of large detuning, the population transfers between the target states are both nonleaky and accelerated, which is highly desirable for performing robust and fast quantum information processing.

(ii) Once the microwave drivings $\tilde{\Phi}_p$ and $\tilde{V}_s$ satisfy the two-photon resonance within the present qutrit, there will never be other two-photon resonance caused by these two drivings. Then the wanted population transfer can be implemented only within the considered qutrit, and thus the leakage errors can be removed effectively.

(iii) Our protocol addresses the direct coupling between $|g\rangle$ and $|a\rangle$ by a microwave flux bias $\tilde{\Phi}_p$, which is different from [27], indirectly inducing states conversion between $|g\rangle$ and $|a\rangle$ by a two-step operation based on the electrical dipole interaction. Thus the present scheme could provide a simplified way to coherently control the transmon system.

(iv) After combining a counterdiabatic driving with the original Hamiltonian $H_I$, the method of transitionless quantum driving could speed up the transfer process as well. However, the counterdiabatic driving could give rise to the leakage effects in our model. Differently, the present invariant-based protocol can construct a suitable shortcut that does not need to break down the form of the original Hamiltonian $H_I$, which is preferable for eliminating leakage effects within the transmon system.

In conclusion, we present a feasible scheme for implementing nonleaky and accelerated population transfer within a transmon-type qutrit. Considering the weak level anharmonicity of the artificial atom, we consider the leakage effects on the target population transfer. The qutrit, constituted by the first three levels, can be coupled to the microwave drivings of ac voltage and time-dependent bias flux. In the case of two-photon resonance with a large detuning, we address a $\Lambda$-configuration interaction which is allowed by the level-transition rule. With the available parameters, a nonleaky population transfer can be drastically accelerated via the technique of STA. Moreover, the accelerated transfer is highly robust against decoherence effects. Combining the negligible leakage effect with the faster coherent control, the present protocol could provide a potential approach for investigating optimal population transfer with quantum transmon circuits experimentally.

## ACKNOWLEDGMENTS

This paper is supported by the Aid Project for the Leading Young Teachers in Henan Provincial Institutions of Higher Education of China (Grant No. 2015GGJS-145), the Aid Project for the Leading Young Talents of Xuchang University, the Key Research Project in Universities of Henan Province (Grants No. 16A140049 and No. 16A140034), the Natural Science Foundation of Zhejiang Province under Grant No. LY14A040001, the National Natural Science Foundation of China under Grant No. 11504316, the Natural Science Foundation of Henan Province (Grant No. 162300410237), and the Development Project for Science and Technology of Henan Province (Grant No. 172102210470).

[1] J. Clarke and F. K. Wilhelm, Nature (London) **453**, 1031 (2008).
[2] J. Q. You and F. Nori, Nature (London) **474**, 589 (2011).
[3] M. H. Devoret and R. J. Schoelkopf, Science **339**, 1169 (2013).
[4] J. Tuorila, M. Silveri, M. Sillanpää, E. Thuneberg, Y. Makhlin, and P. Hakonen, Phys. Rev. Lett. **105**, 257003 (2010).
[5] S. E. de Graaf, J. Leppäkangas, A. Adamyan, A. V. Danilov, T. Lindström, M. Fogelström, T. Bauch, G. Johansson, and S. E. Kubatkin, Phys. Rev. Lett. **111**, 137002 (2013).
[6] J. Koch, T. M. Yu, J. Gambetta, A. A. Houck, D. I. Schuster, J. Majer, A. Blais, M. H. Devoret, S. M. Girvin, and R. J. Schoelkopf, Phys. Rev. A **76**, 042319 (2007).
[7] M. P. Weides, J. S. Kline, M. R. Vissers, M. O. Sandberg, D. S. Wisbey, B. R. Johnson, T. A. Ohki, and D. P. Pappas, Appl. Phys. Lett. **99**, 262502 (2011).
[8] C. Rigetti, J. M. Gambetta, S. Poletto, B. L. T. Plourde, J. M. Chow, A. D. Córcoles, J. A. Smolin, S. T. Merkel, J. R. Rozen, G. A. Keefe, M. B. Rothwell, M. B. Ketchen, and M. Steffen, Phys. Rev. B **86**, 100506(R) (2012).
[9] J. M. Chow, J. M. Gambetta, A. W. Cross, S. T. Merkel, C. Rigetti, and M. Steffen, New J. Phys. **15**, 115012 (2013).
[10] M. J. Peterer, S. J. Bader, X. Jin, F. Yan, A. Kamal, T. J. Gudmundsen, P. J. Leek, T. P. Orlando, W. D. Oliver, and S. Gustavsson, Phys. Rev. Lett. **114**, 010501 (2015).
[11] Z.-B. Feng, Phys. Rev. A **91**, 032307 (2015).
[12] M. Reagor, W. Pfaff, C. Axline, R. W. Heeres, N. Ofek, K. Sliwa, E. Holland, C. Wang, J. Blumoff, K. Chou, M. J. Hatridge, L. Frunzio, M. H. Devoret, L. Jiang, and R. J. Schoelkopf, Phys. Rev. B **94**, 014506 (2016).
[13] S. Novikov, J. E. Robinson, Z. K. Keane, B. Suri, F. C. Wellstood, and B. S. Palmer, Phys. Rev. B **88**, 060503(R) (2013).
[14] X. Y. Jin, A. Kamal, A. P. Sears, T. Gudmundsen, D. Hover, J. Miloshi, R. Slattery, F. Yan, J. Yoder, T. P. Orlando, S. Gustavsson, and W. D. Oliver, Phys. Rev. Lett. **114**, 240501 (2015).
[15] M. Khezri, E. Mlinar, J. Dressel, and A. N. Korotkov, Phys. Rev. A **94**, 012347 (2016).
[16] R. Bianchetti, S. Filipp, M. Baur, J. M. Fink, C. Lang, L. Steffen, M. Boissonneault, A. Blais, and A. Wallraff, Phys. Rev. Lett. **105**, 223601 (2010).
[17] P. J. Liebermann and F. K. Wilhelm, Phys. Rev. Appl. **6**, 024022 (2016).
[18] S. E. Economou and E. Barnes, Phys. Rev. B **91**, 161405(R) (2015).
[19] Z.-B. Feng and M. Li, Opt. Commun. **319**, 56 (2014).
[20] F. Motzoi, J. M. Gambetta, P. Rebentrost, and F. K. Wilhelm, Phys. Rev. Lett. **103**, 110501 (2009).
[21] R. Schutjens, F. A. Dagga, D. J. Egger, and F. K. Wilhelm, Phys. Rev. A **88**, 052330 (2013).
[22] Z. Chen, J. Kelly, C. Quintana, R. Barends, B. Campbell, Y. Chen, B. Chiaro, A. Dunsworth, A. G. Fowler, E. Lucero, E. Jeffrey, A. Megrant, J. Mutus, M. Neeley, C. Neill, P. J. J. O'Malley, P. Roushan, D. Sank, A. Vainsencher, J. Wenner, T. C. White, A. N. Korotkov, and J. M. Martinis, Phys. Rev. Lett. **116**, 020501 (2016).
[23] K. Bergmann, H. Theuer, and B. W. Shore, Rev. Mod. Phys. **70**, 1003 (1998).
[24] P. Král, I. Thanopulos, and M. Shapiro, Rev. Mod. Phys. **79**, 53 (2007).
[25] J. Siewert, T. Brandes, and G. Falci, Opt. Commun. **264**, 435 (2006).
[26] X. Wei and M.-F. Chen, Quantum Inf. Process. **14**, 2419 (2015).
[27] K. S. Kumar, A. Vepsalainen, S. Danilin, and G. S. Paraoanu, Nat. Commun. **7**, 10628 (2016).
[28] C.-P. Yang, J. Phys. A **45**, 205304 (2012).
[29] R. Li, M. Hoover, and F. Gaitan, Quantum Inf. Comput. **9**, 290 (2009).
[30] A. A. Abdumalikov Jr, J. M. Fink, K. Juliusson, M. Pechal, S. Berger, A. Wallraff, and S. Filipp, Nature (London) **496**, 482 (2013).
[31] S.-Y. Huang and H.-S. Goan, Phys. Rev. A **90**, 012318 (2014).
[32] Y. Wang, C. Guo, G.-Q. Zhang, G. Wang, and C. Wu, Sci. Rep. **7**, 44251 (2017).

[33] A. Baksic, H. Ribeiro, and A. A. Clerk, Phys. Rev. Lett. **116**, 230503 (2016).
[34] X. Chen, I. Lizuain, A. Ruschhaupt, D. Guèry-Odelin, and J. G. Muga, Phys. Rev. Lett. **105**, 123003 (2010).
[35] X. Chen, E. Torrontegui, and J. G. Muga, Phys. Rev. A **83**, 062116 (2011).
[36] M. Demirplak and S. A. Rice, J. Phys. Chem. A **107**, 9937 (2003); J. Phys. Chem. B **109**, 6838 (2005).
[37] M. V. Berry, J. Phys. A **142**, 365303 (2009).
[38] S. Masuda and S. A. Rice, J. Phys. Chem. A **119**, 3479 (2015); J. Phys. Chem. C **119**, 14513 (2015).
[39] Y.-C. Li and X. Chen, Phys. Rev. A **94**, 063411 (2016).
[40] A. Ruschhaupt, X. Chen, D. Alonso, and J. G. Muga, New J. Phys. **14**, 093040 (2012).
[41] X. Chen and J. G. Muga, Phys. Rev. A **86**, 033405 (2012).
[42] S. Martínez-Garaot, E. Torrontegui, X. Chen, and J. G. Muga, Phys. Rev. A **89**, 053408 (2014).
[43] X.-J. Lu, X. Chen, A. Ruschhaupt, D. Alonso, S. Guérin, and J. G. Muga, Phys. Rev. A **88**, 033406 (2013).
[44] X.-J. Lu, X. Chen, J. Alonso, and J. G. Muga, Phys. Rev. A **89**, 023627 (2014).
[45] Y.-H. Kang, Y.-H. Chen, Q.-C. Wu, B.-H. Huang, J. Song, and Y. Xia, Sci. Rep. **6**, 36737 (2016).
[46] X. Zhang, Y.-H. Chen, Q.-C. Wu, Z.-C. Shi, J. Song, and Y. Xia, Laser Phys. **27**, 015202 (2017).
[47] Z.-B. Feng and R. Y. Yan, Physica C **492**, 138 (2013).
[48] Z.-L. Shao and Z.-B. Feng, Opt. Commun. **364**, 185 (2016).
[49] S. N. Shevchenko, A. S. Kiyko, A. N. Omelyanchouk, and W. Krech, Low Temp. Phys. **31**, 569 (2005).
[50] G.-J. Gao, X.-H. Zheng, and Z.-L. Cao, Chin. Phys. Lett. **24**, 2733 (2007).
[51] V. V. Shamshutdinova, A. S. Kiyko, S. N. Shevchenko, B. F. Samsonov, and A. N. Omelyanchouk, Russ. Phys. J. **51**, 578 (2008).
[52] N. V. Vitanov and S. Stenholm, Phys. Rev. A **55**, 648 (1997).
[53] H. R. Lewis and W. B. Riesenfeld, J. Math. Phys. **10**, 1458 (1969).
[54] Z.-B. Feng, H.-L. Wang, and R.-Y. Yan, Quantum Inf. Process **15**, 3151 (2016).
[55] J. A. Schreier, A. A. Houck, J. Koch, D. I. Schuster, B. R. Johnson, J. M. Chow, J. M. Gambetta, J. Majer, L. Frunzio, M. H. Devoret, S. M. Girvin, and R. J. Schoelkopf, Phys. Rev. B **77**, 180502(R) (2008).